Recent Results from Dalitz Plot Analysis in D/D_s Decays

A. Palano[1]
[1]INFN and University of Bari, Italy

Introduction

Dalitz plot analysis is an excellent way to study the dynamics of three-body charm decays. These decays are expected to proceed predominantly through intermediate quasi-two-body modes [1] and experimentally this is the observed pattern. Dalitz plot analyses can provide new information on the resonances that contribute to the observed three-body final states. In addition, since the intermediate quasi-two-body modes are dominated by light quark meson resonances, new information on light meson spectroscopy can be obtained. Therefore D meson is as a unique "laboratory" to study light quark spectroscopy. It has a well defined spin-parity $J^P = 0^-$, constraining the angular momentum of the decay products in multibody final states which can be analyzed with the Dalitz plot technique [2].

Investigations of the low mass scalar mesons can be pursued in three-body decays of pseudoscalar D mesons giving their large coupling to such states. The nature of such low mass scalar states is still under discussion [3], since scalar mesons are difficult to resolve experimentally because of their large decay width. There are claims for the existence of broad states close to threshold such as $\kappa(800)$ [4] and $\sigma(600)$ [5]. On the theory side the scalar meson candidates are too numerous to fit in a single $J^{PC} = 0^{++}$ $q\bar{q}$ nonet and therefore alternative interpretations are proposed. For instance, $a_0(980)$ or $f_0(980)$ may be 4-quark states due to their proximity to the $\bar{K}K$ threshold [6]. Table 1 summarize the list of candidates scalar resonances below 2 GeV/c^2. These hypotheses can be tested through

Table 1: Scalar mesons below 2 GeV/c^2.

I = 1/2	I = 1	I = 0
$k(800)$		$\sigma(600)$
	$a_0(980)$	$f_0(980)$
		$f_0(1370)$
$K_0^*(1430)$	$a_0(1490)$	$f_0(1500)$
		$f_0(1700)$
$K_0^*(1950)$		

an accurate measurement of branching fractions and couplings to different final states. In addition, comparison between the production of these states in decays of differently flavored charmed mesons $D^0(c\bar{u})$, $D^+(c\bar{d})$ and $D_s^+(c\bar{s})$ [7] can yield new information on their possible quark composition. Another benefit of studying charm decays is that, in some cases, partial wave analyses are able to isolate the scalar contribution almost background free.

Results of D^0 Dalitz analyses can be an input for extracting the CP-violating phase $\gamma = \arg(-V_{ud}V_{ub}^*/V_{cd}V_{cb}^*)$ of the quark mixing matrix by exploiting interference structure in the Dalitz plot from the decay $B^\pm \to D^0 K^\pm$ [8]. Modeling of the $K\pi$ and $\pi\pi$ S-wave in D decays is therefore an important element in such measurement, since the systematic uncertainty on γ due to the Dalitz model is dominated by such components [9].

Some states need to be described by a coupled channel formalism. Broad overlapping resonances cannot be described by standard Breit-Wigner's. It is therefore necessary to have appropriate description of the resonances involved in the charmed meson decay. On the other hand, the decay itself can be used, in some cases, to extract new clean information on the lineshape and parameters of these resonances. Four different approaches have been developed.

- Isobar model;
- K-matrix formalism;
- Model Independent Partial Wave Analysis;
- Direct Partial Wave Analysis.

Dalitz analysis formalism

The amplitudes describing D meson weak-decays into three-body final states are dominated by intermediate resonances that lead to highly non-uniform intensity distributions in the available phase space.

Neglecting CP violation in D meson decays, we define the D decay amplitude $\mathcal{A}$ in a $D \to ABC$ Dalitz plot, as:

$$\mathcal{A}[D \to ABC] \equiv f(m_{BC}^2, m_{AC}^2). \quad (1)$$

The complex quantum mechanical amplitude f is a coherent sum of all relevant quasi-two-body $D \to (r \to AB)C$ resonances ("isobar model" [10]), $f = \sum_r a_r e^{i\phi_r} A_r(s)$. Here $s = m_{AB}^2$, and A_r is the resonance amplitude. Each amplitude A_r is represented by the product of a complex Breit-Wigner $BW(m)$ and a real angular term:

$$A_r = BW(m) \times T(\Omega). \quad (2)$$

The Breit-Wigner functions include the Blatt-Weisskopf form factors [11]. The angular terms $T(\Omega)$ are described in Ref. [12]. The coefficients a_r and ϕ_r are usually obtained from a likelihood fit. The probability density function for the signal events is $|f|^2$. Sub-modes branching fractions ("fit fractions") are defined as

$$f_r = \frac{|a_r|^2 \int |A_r|^2 dm_{AC}^2 dm_{BC}^2}{\sum_{j,r} c_j c_r^* \int A_j A_r^* dm_{AC}^2 dm_{BC}^2}. \quad (3)$$

The fractions f_r do not necessarily add up to 1 because of interference effects among the amplitudes.

Study of $D^0 \to \bar{K}^0\pi^+\pi^-$

The $D^0 \to \bar{K}^0\pi^+\pi^-$ final state has been extensively studied in the framework of the measurement of γ by *BABAR* [9] and Belle [13] experiments. The data sample used in the *BABAR* analysis corresponds to an integrated luminosity of 351 fb^{-1} recorded at the SLAC PEP-II storage rings, operating at center of mass energies near the $\Upsilon(4S)$ resonance.

Two different models have been used in this analysis. The first model (also referred to as Breit-Wigner or isobar model) [14] expresses $\mathcal{A}_r$ as a sum of two-body decay-matrix elements and a non-resonant contribution. In the second model (hereafter referred to as the $\pi\pi$ S-wave K-matrix model) the treatment of the $\pi\pi$ S-wave states in $D^0 \to K^0_S\pi^-\pi^+$ uses a K-matrix formalism [15, 16] to account for the non-trivial dynamics due to the presence of broad and overlapping resonances. The two models have been obtained using a high statistics flavor tagged D^0 sample ($D^{*+} \to D^0\pi^+_s$) selected from $e^+e^- \to c\bar{c}$ events.

In the Breit-Wigner model a set of several two-body amplitudes is used, including five Cabibbo-allowed amplitudes: $K^*(892)^+\pi^-$, $K^*(1410)^+\pi^-$, $K^*_0(1430)^+\pi^-$, $K^*_2(1430)^+\pi^-$ and $K^*(1680)^+\pi^-$, their doubly Cabibbo-suppressed partners, and eight channels with a K^0_S and a $\pi\pi$ resonance: ρ, ω, $f_0(980)$, $f_2(1270)$, $f_0(1370)$, $\rho(1450)$ and two "ad-hoc" scalar resonances: σ_1 and σ_2 . The Breit–Wigner masses and widths of the scalars σ_1 and σ_2 are left unconstrained, while the parameters of the other resonances are taken from PDG [12]. The parameters of the σ resonances obtained in the fit are as follows: $M_{\sigma_1} = 528 \pm 5$ MeV/c^2, $\Gamma_{\sigma_1} = 512 \pm 9$ MeV/c^2, $M_{\sigma_2} = 1033 \pm 4$ MeV/c^2 and $\Gamma_{\sigma_2} = 99 \pm 6$ MeV/c^2 (the errors are statistical only). The amplitudes are measured with respect to $D^0 \to K^0_S\rho(770)^0$ which gives the second largest contribution. The $K\pi$ and $\pi\pi$ P-waves dominate the decay, but significant contributions from the corresponding S-waves are also observed (above 6 and 4 standard deviations, respectively).

The alternative model is based on a fit to scattering data (K-matrix [17]) used to parametrize the $\pi\pi$ S-wave component.

In the *BABAR* analysis performed with the K-matrix model, the sum of fit fractions is $(103.6 \pm 5.2)\%$, and the goodness of fit is estimated through a two-dimensional χ^2 test performed binning the Dalitz plot into square regions of size 0.015 GeV$^2/c^4$, yielding a reduced χ^2 of 1.11 (including statistical errors only) for 19274 degrees of freedom. The resulting fractions are shown in Table 2. The variation of the contribution to the χ^2 as a function of the Dalitz plot position is approximately uniform. Figure 1(a,b,c) shows the Dalitz fit projections overlaid with the data distributions. The Dalitz plot distributions are well reproduced, with some small discrepancies in low and high mass regions of the m^2_0 projection, and in the $\rho(770)^0 - \omega(782)$ interference region.

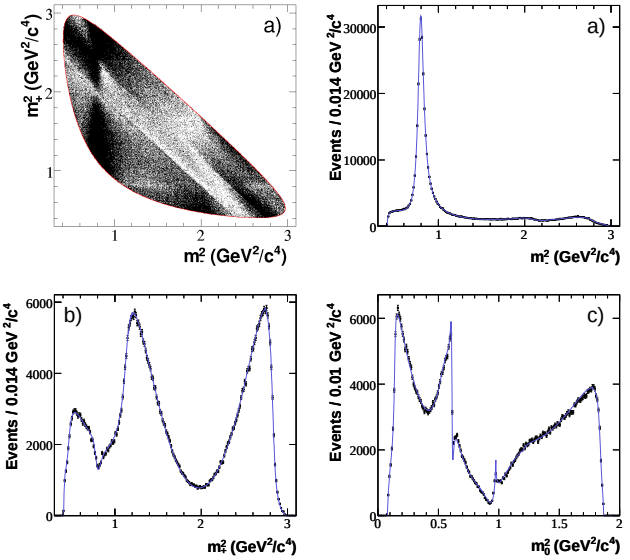

Figure 1: *BABAR*. The $\bar{D}^0 \to K^0_S\pi^-\pi^+$ Dalitz distribution and projections on (a) $m^2_+ = m^2_{K^0_S\pi^+}$, (b) $m^2_- = m^2_{K^0_S\pi^-}$, and (c) $m^2_{\pi^+\pi^-}$. The curves are the K-matrix model fit projections.

The isobar model, on the other hand, gives a sum of fit fractions of 122.5%, and a reduced χ^2 of 1.20 (with statistical errors only), which strongly disfavors the isobar approach in comparison to the K-matrix formalism.

Study of $D^+ \to \pi^+\pi^-\pi^+$ and the $\sigma(600)$

A study of charged D decay to three charged pions has been carried out with the CLEO detector [18]. This mode has been studied previously by E687 [19], E691 [20], E791 [5], and FOCUS [21].

E791 uses the isobar technique, where each resonant contribution to the Dalitz plot is modeled as a Breit-Wigner amplitude with a complex phase. This works well for narrow, well separated resonances, but when the resonances are wide and start to overlap, solutions become ambiguous, and unitarity is violated. In contrast, FOCUS uses the K-matrix approach. The two techniques give a good description of the observed Dalitz plots and agree about the overall contributions of the resonances. Both experiments see that about half of the fit fraction for this decay is explained by a low $\pi^+\pi^-$ mass S wave.

The CLEO analysis utilizes 281 pb^{-1} of data collected on the $\psi(3770)$ resonance at $\sqrt{s} \simeq$3773 MeV at the Cornell Electron Storage Ring, corresponding to a production of about 0.78×10^6 D^+D^- pairs. D^+ mesons are produced close to the threshold, and are thus almost at rest. Events from the decay $D^+ \to K^0_S\pi^+$, which has a large rate and contributes to the same final state, are isolated with the

Table 2: *BABAR*. Amplitudes and fit fractions as obtained from the fit of the $D^0 \to K^0_S\pi^+\pi^-$ Dalitz plot distribution using the K-matrix formalism. Errors for amplitudes are statistical only, while for fit fractions include statistical and systematic uncertainties, largely dominated by the latter. Upper limits on fit fractions are quoted at 95% confidence level.

Component	a_r	ϕ_r (deg)	Fraction (%)
$K^*(892)^-$	1.740 ± 0.010	139.0 ± 0.3	55.7 ± 2.8
$K^*_0(1430)^-$	8.2 ± 0.7	153 ± 8	10.2 ± 1.5
$K^*_2(1430)^-$	1.410 ± 0.022	138.4 ± 1.0	2.2 ± 1.6
$K^*(1680)^-$	1.46 ± 0.10	-174 ± 4	0.7 ± 1.9
$K^*(892)^+$	0.158 ± 0.003	-42.7 ± 1.2	0.46 ± 0.23
$K^*_0(1430)^+$	0.32 ± 0.06	143 ± 11	< 0.05
$K^*_2(1430)^+$	0.091 ± 0.016	85 ± 11	< 0.12
$\rho(770)^0$	1	0	21.0 ± 1.6
$\omega(782)$	0.0527 ± 0.0007	126.5 ± 0.9	0.9 ± 1.0
$f_2(1270)$	0.606 ± 0.026	157.4 ± 2.2	0.6 ± 0.7
$\pi\pi$ S-wave			11.9 ± 2.6

$\pi^+\pi^-$ invariant mass even without clearly detached vertexes as in the fixed target experiments. They obtain, for the Dalitz plot analysis, 4086 events $\sim$2600 of which are signal events.

An isobar model is used to parametrize the signal decay where the description of the σ from Ref. [22] and the Flatté parameterization for the threshold effects on the $f_0(980)$ [23] (with parameters taken from the recent BES II measurement [24]) are included. Alternative models are also tried and give comparably good fit results [25] [26].

CLEO-c was able to reproduce the fit results E791 [5]. The amplitude normalization and sign conventions are different from E791, in particular the inclusion of a $\sigma\pi$ contribution gives a fit probability of $\simeq 20\%$. Possible contributions form all known $\pi^+\pi^-$ resonances listed in Ref. [12] were tried, including high mass resonances giving asymptotic "tails" at the edge of the kinematically allowed region. For the σ a complex pole amplitude, was eventually tried rather than the spin-0 Breit-Wigner.

Table 3 shows the list of surviving contributions with their fitted amplitudes and phases, and calculated fit fractions after a procedure of addition and removal of resonances to improve the consistency between the model and data. The sum of all fit fractions is 90.1%, and the fit probability is $\simeq$28% for 90 degrees of freedom. The projection of the Dalitz plot and selected fit components onto the $m^2(\pi^+\pi^-)$ axis is shown in Fig. 2. For the poorly established resonances as the σ pole, their parameters are allowed to float and the variations of the other fit parameters contribute to the systematic errors. The fitted values for the σ pole are $Re(m_\sigma)$ (MeV/c^2) = 466$\pm$18 and $Im(m_\sigma)$ (MeV/c^2) = –223$\pm$28.

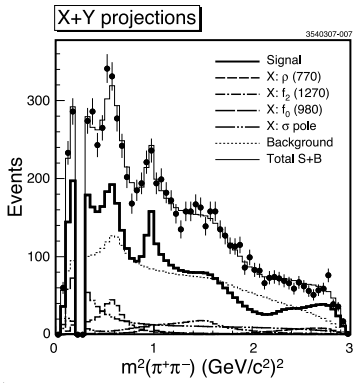

Figure 2: Projection of the Dalitz plot onto the $m^2(\pi^+\pi^-)$ axis (two combinations per D^+ candidate) for CLEO-c data (points) and isobar model fit (histograms) showing the various components.

Study of $D^+ \to K^-\pi^+\pi^+$ and the $K\pi$ S-wave

The most detailed experimental information on the $K\pi$ S-wave comes from studies of $D^+ \to K^-\pi^+\pi^+$ decays. These Cabibbo favored decays are known to contain a large S-wave component.

A study of $\sim 15,000$ such decays by the E791 collaboration [4] provides an illustration. The E791 Dalitz plot is shown in Fig. 3 where significant S-P interference is evident from the asymmetry of the $K^*(890)$ bands.

Isobar Model Fits. In the earliest analyses of these decays, a model with interfering resonances like the $K^*(890)$, the $L = 0$ $K^*_0(1430)$ and a constant non-resonant "NR" 3-body amplitude could account for the voids and asymmetries observed in the Dalitz plot. With their larger sample, the E791 isobar model analysis showed that additional structure in the S-wave was required to achieve an acceptable fit, and the addition of a $\kappa(800)$ Breit-Wigner isobar, which interfered destructively with the NR term, worked well.

The "isobar model" description of the $L = 0, 1$ and 2

Table 3: CLEO-c. Results of the isobar model analysis of the $D^+ \to \pi^-\pi^+\pi^+$ Dalitz plot. For each contribution the relative amplitude, phase, and fit fraction is given. The errors are statistical and systematic, respectively.

Mode	Amplitude (a.u.)	Phase (°)	Fit fraction (%)
$\rho(770)\pi^+$	1(fixed)	0(fixed)	20.0±2.3±0.9
$f_0(980)\pi^+$	1.4±0.2±0.2	12±10±5	4.1±0.9±0.3
$f_2(1270)\pi^+$	2.1±0.2±0.1	–123±6±3	18.2±2.6±0.7
$f_0(1370)\pi^+$	1.3±0.4±0.2	–21±15±14	2.6±1.8±0.6
$f_0(1500)\pi^+$	1.1±0.3±0.2	–44±13±16	3.4±1.0±0.8
σ pole	3.7±0.3±0.2	–3±4±2	41.8±1.4±2.5

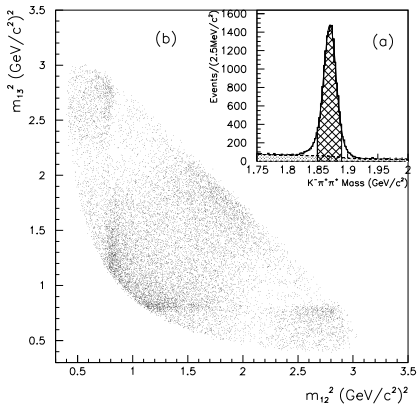

Figure 3: E791. Dalitz plot for $D^+ \to K^-\pi^+\pi^+$ decays. The figure and show distributions of squared invariant mass for one $K^-\pi^+$ combination plotted against the other (symmetrized).

wave amplitudes F_L in the $K^-\pi^+$ systems for this fit can be summarized as:

$$\begin{aligned} F_0(s) &= \alpha_{00} + \alpha_{10} BW_{K_0^*(1430)}(s) \\ &\quad + \alpha_{20} BW_{\kappa(800)}(s) \qquad (4) \\ F_1(s) &= \alpha_{11} BW_{K_1^*(890)}(s) \\ &\quad + \alpha_{21} BW_{K_0^*(1688)}(s) \qquad (5) \\ F_2(s) &= \alpha_{21} BW_{K_2^*(140)} \qquad (6) \end{aligned}$$

where the $BW(s)$ are relativistic Breit-Wigner functions with s-dependent widths, and the α_{iL} are complex coefficients determined in the fit. The overall phase was defined by setting $\alpha_{11} = 1.0$, and α_{00} was the NR term.

Two further isobar model analyses of this decay mode were recently made, one by FOCUS [27] and the other by CLEO-c [28]. Each used samples ~ 3.5 times larger. The conclusions, and estimates of the resonant fractions of both were in good general agreement with E791.

Parameters for κ and $K_0^*(1430)$ S-wave Breit Wigner isobars are compared for the three experiments in Table 4. The $K_0^*(1430)$ parameters in this model disagree significantly with those obtained by the LASS [29] experiment or with the World average [12]. There is general agreement that this description of the S-wave, described by Eq. (4), with two broad, Breit Wigner resonances, one of which is also near threshold, is theoretically problematic and could account for this discrepancy. It would be virtually certain that this amplitude would have an s-dependent phase that would differ from the Watson theorem expectation.

Model-Independent Measurement. A test of the Watson theorem requires a measurement of the phase of $F(s)$ at several values of s in a model-independent way. The first attempt to do this for the S-wave for $K^-\pi^+$ produced in this decay mode was made by the E791 collaboration [30].

They replaced the analytical function describing the S-wave in Eq. (4) by a set of 38 complex values at discrete values for s, using a spline interpolation for other values. The P- and D-waves were parametrized, as before, by the form in Eqs. (5) and (6) and the coefficients α_{iL} were allowed to float. A fit was then made to determine the best values (magnitude and phase) for each of the 38 S-wave points. The result, shown in Fig. 4, is compared with the LASS model for the $I = 1/2$ $K^-\pi^+$ system. Agreement is good in the $K_0^*(1430)$ region (above $\sim$1100 MeV/c^2) after a shift in phase of 75° and an arbitrary scale factor are applied to the LASS amplitude. A very significant discrepancy is, however, seen for lower values of invariant mass.

However there are two problems. First, though $I = 1/2$ $K^-\pi^+$ production probably dominates, $I = 3/2$ production in these decays cannot be excluded. Second, the isobar model form in Eqs. (5) and (6) for the P- and D-waves, upon which this result depends, is questionable. The P-wave contains more than one Breit-Wigner, and both waves are assumed to be dominated by resonant behavior. More importantly, neither wave is likely to follow the Watson theorem, so a test of the S-wave alone cannot be conclusive.

The CLEO collaboration [28] has attempted to overcome the latter difficulty. Using their high purity sample of $\sim 60,000$ events, they proceeded in the same way as E791, interpolating the S-wave between discrete values of s, while parameterizing the P- and D-waves as above. Their results were very similar. They then fixed the S-wave and, using a similar procedure, fit the $P-$wave parametrized in the same way. Then they repeated this for

Table 4: Breit Wigner Parameters for the $K^-\pi^+$ S-wave Isobar States. All quantities are in MeV/c^2.

		E791	Focus	CLEO c	PDG
κ	$M_\circ$	$797 \pm 19 \pm 42$	883 ± 13	805 ± 11	672 ± 40
	$\Gamma_\circ$	$410 \pm 43 \pm 85$	355 ± 13	453 ± 21	550 ± 34
$K^*_\circ$	$M_\circ$	$1459 \pm 7 \pm 12$	1461 ± 4	1461 ± 3	1414 ± 6
	$\Gamma_\circ$	$175 \pm 12 \pm 12$	177 ± 8	169 ± 5	290 ± 21

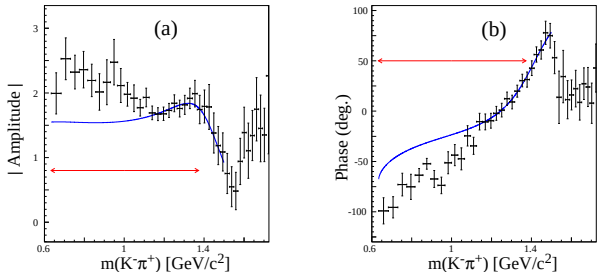

Figure 4: (a) Magnitude and (b) phase of the decay amplitude $F_0(s)$ at 38 discrete values of s (squared invariant mass of the $K^-\pi^+$ systems from $D^0 \to K^-\pi^+\pi^+$ decays taken from Ref. [30]. The LASS model shifted by -75° and scaled to the region where $s > 1.2$ (GeV/c^2)^2 is shown as the blue, continuous curve.

the D-wave. In each step, only one wave was allowed to float with the others fixed. The analysis makes also use of the I=2 contribution.

This procedure can converge only by simultaneously floating all waves at once, and this was not done. Also, the phases have to be defined in some part of the phase space (as little as possible) in order for this to work.

Study of $D_s^+ \to \pi^+\pi^-\pi^+$ and the $f_0(980)$

This analysis was performed by *BABAR* [31] and focuses on the study of the three-body D_s^+ meson decays to $\pi^+\pi^-\pi^+$ and performs, for the first time, a Model-Independent Partial Wave Analysis (MIPWA). Previous Dalitz plot analyses of this decay mode were based on much smaller data samples [32, 33].

The combinatorial background is reduced by requiring the D_s^+ to originate from the decay

$$D_s^*(2112)^+ \to D_s^+\gamma \qquad (7)$$

and by using geometrical+kinematical variables combined in a likelihood ratio test. The cut on the likelihood ratio has been chosen in order to obtain the largest statistics with background small enough to perform a Dalitz plot analysis. The signal region contains 13179 events with a purity of 80%. The resulting Dalitz plot, symmetrized along the two axes, is shown in Fig. 5(b). They observe a clear $f_0(980)$ signal, evidenced by the two narrow crossing bands. There is also a broad accumulation of events in the 1.9 GeV$^2/c^4$ region.

An unbinned maximum likelihood fit is performed on the distribution of events in the Dalitz plot to determine the relative amplitudes and phases of intermediate resonant and nonresonant states. The phase of each amplitude (*i.e.* the phase of the corresponding c_i) is measured with respect to the $f_2(1270)\pi^+$ amplitude.

For the $\pi^+\pi^-$ $\mathcal{S}$-wave amplitude they use the Model-Independent Partial Wave Analysis: instead of including the $\mathcal{S}$-wave amplitude as a superposition of relativistic Breit-Wigner functions, they divide the $\pi^+\pi^-$ mass spectrum into 29 slices and they parametrize the $\mathcal{S}$-wave by an interpolation between the 30 endpoints in the complex plane:

$$A_{\mathcal{S}-\mathrm{wave}}(m_{\pi\pi}) = \mathrm{Interp}(c_k(m_{\pi\pi})e^{i\phi_k(m_{\pi\pi})})_{k=1,..,30}. \qquad (8)$$

The amplitude and phase of each endpoint are free parameters. Interpolation is implemented by a Relaxed Cubic Spline. The phase is not constrained in a specific range in order to allow the spline to be a continuous function.

The resulting $\mathcal{S}$-wave $\pi^+\pi^-$ amplitude and phase is shown in Fig. 5(a),(b). The fitted fractions are given in Table 5.

Table 5: *BABAR*. Results from the $D_s^+ \to \pi^+\pi^-\pi^+$ Dalitz plot analysis. The table reports the fit fractions. Errors are statistical and systematic respectively.

Decay Mode	Decay fraction(%)
$f_2(1270)\pi^+$	$10.1 \pm 1.5 \pm 1.0$
$\rho(770)\pi^+$	$1.8 \pm 0.5 \pm 1.0$
$\rho(1450)\pi^+$	$2.3 \pm 0.8 \pm 1.7$
$\mathcal{S}$-wave	$83.0 \pm 0.9 \pm 1.9$
Total	$97.2 \pm 3.7 \pm 3.8$
χ^2/NDF	$\frac{437}{422-64} = 1.2$

The results from the Dalitz plot analysis can be summarized as follows:

- The decay is dominated by the $D_s^+ \to (\pi^+\pi^-)_{\mathcal{S}-\mathrm{wave}}\pi^+$ contribution.

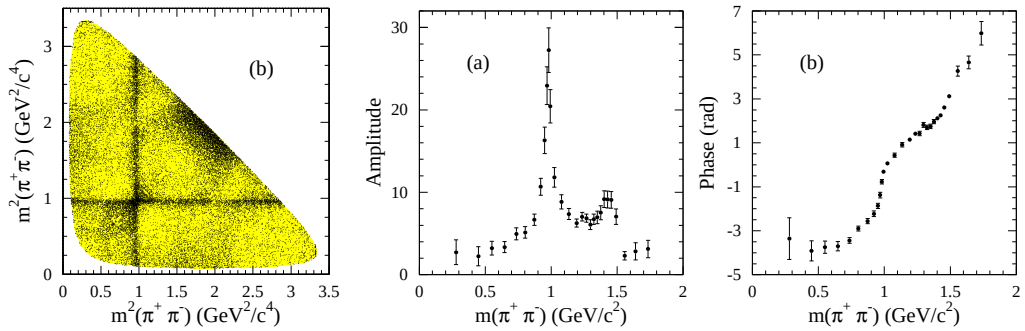

Figure 5: *BABAR*. $D_s^+ \to \pi^+\pi^-\pi^+$ Dalitz plot. Right. (a) $\mathcal{S}$-wave amplitude extracted from the best fit, (b) corresponding $\mathcal{S}$-wave phase. Errors are statistical only.

- The $\mathcal{S}$-wave shows, in both amplitude and phase, the expected behavior for the $f_0(980)$ resonance.
- The $\mathcal{S}$-wave shows further activity, in both amplitude and phase, in the regions of the $f_0(1370)$ and $f_0(1500)$ resonances.
- The $\mathcal{S}$-wave is small in the $\sigma/f_0(600)$ region, indicating that this resonance has a small coupling to $s\bar{s}$.
- There is an important contribution from $D_s^+ \to f_2(1270)\pi^+$ whose size is in agreement with that reported by FOCUS, but a factor two smaller than that reported by E791. This is the largest contribution in charm decays from a spin-2 resonance.

Study of $D_s^+ \to K^+K^-\pi^+$

This *BABAR* analysis makes use of an integrated luminosity of 240 fb^{-1}. Events are selected in a sample of events having at least three reconstructed charged tracks with two well identified kaons and one pion. The decay chain $D_s^*(2112)^+ \to D_s^+\gamma$ helps in discriminating signal from combinatorial background. Additional requirements based on kinematic and geometric information are combined to further suppress the background. The final sample contains 100850 events with a purity of 95%. An unbinned maximum likelihood fit of the Dalitz plot (Fig.6) is performed to extract the relative amplitudes and phases of the intermediate resonances as shown in Table 6. The decay is dominated by the $\phi(1020)\pi^+$ and $f_0(980)\pi^+$. The $f_0(980)$ is parametrized with a coupled channel Breit-Wigner [24] and its contribution is large but it is subject to a large systematic error due to the poor knowledge of its parameters and possible $a_0(980)$ contributions that are difficult to disentangle in the $K\bar{K}$ projection.

Analysis of the angular moment distribution confirms such picture with a big S-wave–P-wave interference in the $K\bar{K}$ channel in the region of the $\phi(1020)$. On the other hand very small activity is present in the $K^*(892)$ region suggesting a small $K\pi$ S-wave, and therefore no evidence of a $\kappa(800)$.

Figure 6: *BABAR*. Dalitz plot analysis of $D_s^+ \to \pi^+K^+K^-$

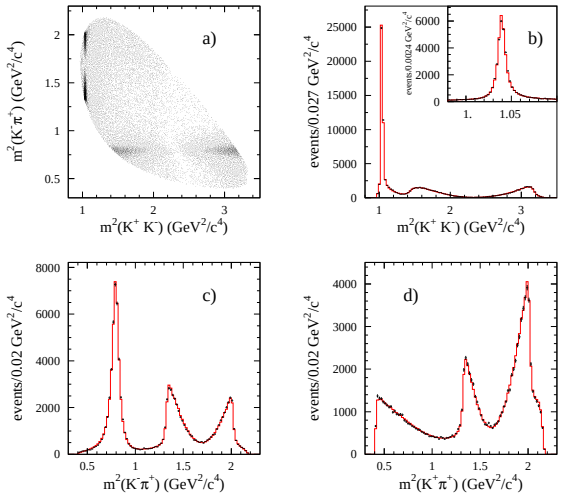

A similar analysis has been recently performed by CLEO [34] using 14400 events.

Study of $D^0 \to \bar{K}^0K^-K^+$ and the $a_0(980)$ resonance

The data sample used in the *BABAR* $D^0 \to \bar{K}^0K^-K^+$ analysis consists of 91.5 fb^{-1} [35]. Selecting events within $\pm 2\sigma$ of the fitted D^0 mass value, a signal fraction of 97.3% is obtained for the 12540 events selected. The Dalitz plot for these $D^0 \to \overline{K}^0K^+K^-$ candidates is shown in Fig. 7.

In the K^+K^- threshold region, a strong $\phi(1020)$ signal is observed, together with a rather broad structure. A large asymmetry with respect to the $\overline{K}^0K^+$ axis can also be seen in the vicinity of the $\phi(1020)$ signal, which is most probably the result of interference between S and P-wave amplitude contributions to the K^+K^- system. The $f_0(980)$ and $a_0(980)$ S-wave resonances are, in fact, just below the K^+K^- threshold, and might be expected to contribute in the vicinity of $\phi(1020)$. An accumulation of events due

Mode	Amplitude (a.u.)	Phase (°)	Fit fraction (%)
$K^*(892)K^+$	1(fixed)	0(fixed)	$48.7 \pm 0.2 \pm 1.6$
$\phi(1020)\pi^+$	$1.081 \pm 0.006 \pm 0.049$	$2.56 \pm 0.02 \pm 0.38$	$37.9 \pm 0.2 \pm 1.8$
$f_0(980)\pi^+$	$4.6 \pm 0.1 \pm 1.6$	$-1.04 \pm 0.04 \pm 0.48$	$35 \pm 1 \pm 14$
$K_0^*(1430)^0K^+$	$1.07 \pm 0.06 \pm 0.73$	$-1.37 \pm 0.05 \pm 0.81$	$2.0 \pm 0.2 \pm 3.3$
$f_0(1710)\pi^+$	$0.83 \pm 0.02 \pm 0.18$	$-2.11 \pm 0.05 \pm 0.42$	$2.0 \pm 0.1 \pm 1.0$
$f_0(1370)\pi^+$	$1.74 \pm 0.09 \pm 1.05$	$-2.6 \pm 0.1 \pm 1.1$	$6.3 \pm 0.6 \pm 4.8$
$K_2^*(1430)^0K^+$	$0.43 \pm 0.05 \pm 0.34$	$-2.5 \pm 0.1 \pm 0.3$	$0.17 \pm 0.05 \pm 0.30$
$f_2(1270)\pi^+$	$0.40 \pm 0.04 \pm 0.35$	$0.3 \pm 0.2 \pm 0.5$	$0.18 \pm 0.03 \pm 0.40$
Sum	$132 \pm 1 \pm 16$		

Table 6: *BABAR*. Results of the isobar model analysis of the $D_s^+ \to K^+K^-\pi^+$ Dalitz plot. For each contribution the relative amplitude, phase, and fit fraction is given. The errors are statistical and systematic, respectively.

Table 7: *BABAR*. Results from the Dalitz plot analysis of $D^0 \to \overline{K}^0K^+K^-$.

Final state	Amplitude	Phase (radians)	Fraction (%)
$\overline{K}^0a_0(980)^0$	1.	0.	$66.4 \pm 1.6 \pm 7.0$
$\overline{K}^0\phi(1020)$	$0.437 \pm 0.006 \pm 0.060$	$1.91 \pm 0.02 \pm 0.10$	$45.9 \pm 0.7 \pm 0.7$
$K^-a_0(980)^+$	$0.460 \pm 0.017 \pm 0.056$	$3.59 \pm 0.05 \pm 0.20$	$13.4 \pm 1.1 \pm 3.7$
$\overline{K}^0f_0(1400)$	$0.435 \pm 0.033 \pm 0.162$	-2.63 $\pm$ 0.10 $\pm$ 0 .71	$3.8 \pm 0.7 \pm 2.3$
$\overline{K}^0f_0(980)$			$0.4 \pm 0.2 \pm 0.8$
$K^+a_0(980)^-$			$0.8 \pm 0.3 \pm 0.8$
Sum			$130.7 \pm 2.2 \pm 8.4$

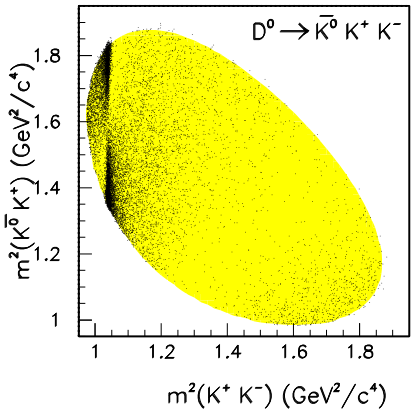

Figure 7: *BABAR*. Dalitz plot of $D^0 \to \overline{K}^0K^+K^-$.

to a charged $a_0(980)^+$ can be observed on the lower right edge of the Dalitz plot. This contribution, however, does not overlap with the $\phi(1020)$ region and this allows the K^+K^- scalar and vector components to be separated using a partial wave analysis in the low mass K^+K^- region.

The helicity angle, θ_K, is then defined as the angle between the K^+ for D^0 (or K^- for $\overline{D}^0$) in the K^+K^- rest frame and the K^+K^- direction in the D^0 (or $\overline{K}^0$) rest frame. The K^+K^- mass distribution has been modified by weighting each D^0 candidate by the spherical harmonic $Y_L^0(\cos\theta_K)$ (L=0-4) divided by its (Dalitz-plot-dependent) fitted efficiency. It is found that all the $\langle Y_L^0 \rangle$ moments are small or consistent with zero, except for $\langle Y_0^0 \rangle$, $\langle Y_1^0 \rangle$ and $\langle Y_2^0 \rangle$.

In order to interpret these distributions a simple partial wave analysis has been performed, involving only S- and P-wave amplitudes. This results in the following set of equations [36]:

$$\sqrt{4\pi}\langle Y_0^0 \rangle = S^2 + P^2 \quad (9)$$

$$\sqrt{4\pi}\langle Y_1^0 \rangle = 2 \mid S \mid\mid P \mid \cos\phi_{SP} \quad (10)$$

$$\sqrt{4\pi}\langle Y_2^0 \rangle = \frac{2}{\sqrt{5}}P^2, \quad (11)$$

where S and P are proportional to the size of the S- and P-wave contributions and ϕ_{SP} is their relative phase. Under these assumptions, the $\langle Y_2^0 \rangle$ moment is proportional to P^2 so that it is natural that the $\phi(1020)$ appears free of background, as is observed.

The above system of equations can be solved directly for S^2, P^2 and $\cos\phi_{SP}$ and corrected for phase space distribution. The phase space corrected spectra are shown in Fig. 8.

The distributions have been fitted using a model with $\phi(1020)$ for the P-wave , a scalar contribution in the K^+K^- mass projection entirely due to the $a_0(980)^0$, $\overline{K}^0K^+$ mass distribution is entirely due to $a_0(980)^+$ and the $\cos\phi_{SP}$ described with BW models.

The $a_0(980)$ scalar resonance has a mass very close to the $\bar{K}K$ threshold and decays mostly to $\eta\pi$. It has been described by a coupled channel Breit Wigner. The fit produces a reasonable representation of the data for all of the projections. The χ^2 computed on the Dalitz plot gives a value of χ^2/NDF=983/774. The sum of the fractions is $130.7 \pm 2.2 \pm 8.4\%$. The regions of higher χ^2 are distributed rather uniformly on the Dalitz plot.

The final fit results showing fractions, amplitudes and phases are summarized in Table 7. For $\overline{K}^0 f_0(980)$ and $K^+ a_0(980)^-$ (DCS), being consistent with zero, only the fractions have been tabulated. For the Dalitz plot analysis the $f_0(980)$ contribution is found to be consistent with zero,

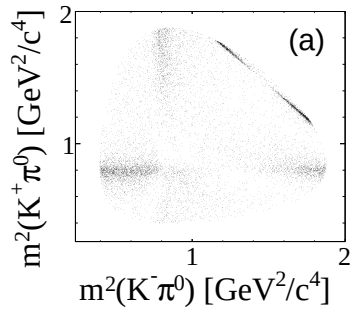

Figure 9: *BABAR*. Dalitz plot for $D^0 \to K^- K^+ \pi^0$.

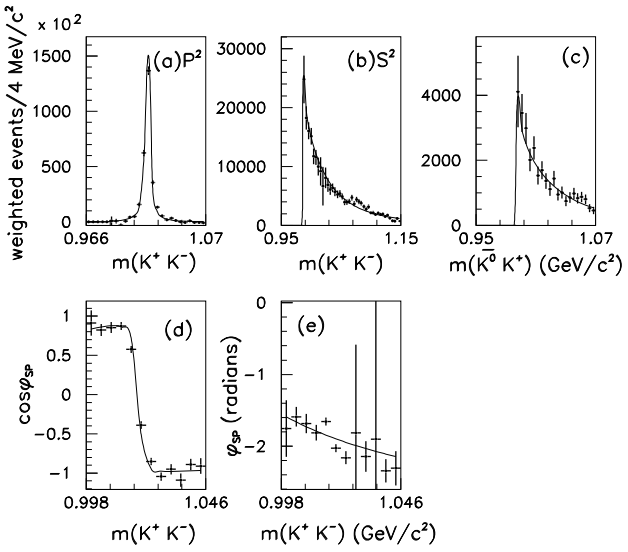

Figure 8: *BABAR*. Results from the K^+K^- Partial Wave Analysis. (a) P-wave strength, (b) S-wave strength. (c) $m(\overline{K}^0 K^+)$ distribution, (d) $\cos\phi_{SP}$ in the $\phi(1020)$ region. (e) ϕ_{SP} in the threshold region after having subtracted the fitted $\phi(1020)$ phase motion shown in (d).

Study of $D^0 \to K^+K^-\pi^0$

BaBar analyzed 385 fb^{-1} of e^+e^- collision data and reconstructed the decays $D^{*+} \to D^0\pi^+$ with $D^0 \to K^-K^+\pi^0$ [37]. Requirements on the center-of-mass momentum of the D^0 candidate yields in the signal region 11278 ± 110 signal events with a purity of about 98.1%.

The results from the Dalitz plot analysis are summarized in Table 8. For D^0 decays to $K^\pm\pi^0$ S-wave states, three amplitude models have been considered. One model uses the LASS amplitude for $K^-\pi^+ \to K^-\pi^+$ elastic scattering [29], A second model uses the E791 results for the $K^-\pi^+$ S-wave amplitude from an energy-independent partial wave analysis in the decay $D^+ \to K^-\pi^+\pi^+$ [30]. The third model uses a coherent sum of a uniform non-resonant term, and Breit-Wigner terms for the $\kappa(800)$ and $K_0^*(1430)$ resonances.

The D^0decay to a K^-K^+ S-wave state is described by a coupled-channel Breit-Wigner amplitude for the $f_0(980)$ and $a_0(980)$ resonances, with their respective couplings to $\pi\pi$, $K\bar{K}$ and $\eta\pi$, $K\bar{K}$ final states [23],

Several models are used incorporating various combinations of intermediate states. In each fit, the $K^*(892)^+$ is included and the complex amplitude coefficients of other states relative to it is measured.

The LASS $K\pi$ S-wave amplitude gives the best agreement with data and it is uses it in the nominal fits. The $K\pi$ S-wave modeled by the combination of $\kappa(800)$ (with parameters taken from Ref. [4]), a non-resonant term and $K_0^*(1430)$ has a smaller fit probability (χ^2 probability $<$ 5%). The best fit with this model (χ^2 probability 13%) yields a charged κ of mass (870 ± 30) MeV/c^2, and width (150 ± 20) MeV/c^2, significantly different from those reported in Ref. [4] for the neutral state. This does not support the hypothesis that production of a charged, scalar κ is being observed. The E791 amplitude [30] describes the data well, except near threshold (χ^2 probability 23%).

The mass dependent K^-K^+ S- and P-wave complex amplitudes can also be obtained directly from our data in a model-independent way in a limited mass range around 1 GeV/c^2. In a region of the Dalitz plot where S- and P-waves in a single channel dominate, their amplitudes are given by the Legendre polynomial moments which have been used to evaluate $|S|$ and $|P|$, shown in Fig. 10, for the K^-K^+ channel in the mass range $m_{K^-K^+} <$ 1.15 GeV/c^2. The measured values of $|S|$ agree well with those obtained in the analysis of the decay $D^0 \to K^-K^+\bar{K}^0$ [35]. They also agree well with either the $f_0(980)$ or the $a_0(980)$ lineshape. The measured values of $|P|$ are consistent with a Breit-Wigner lineshape for $\phi(1020)$.

Table 8: *BABAR*. The results obtained from the $D^0 \to K^-K^+\pi^0$ Dalitz plot fit. The $a_0(980)$ contribution, when it is included in place of the $f_0(980)$, is given in square brackets. The $K\pi$ S-wave states are denoted by $K^{\pm}\pi^0(S)$.

State	Amplitude, a_r	Phase, ϕ_r (°)	Fraction, f_r (%)
$K^*(892)^+$	1.0 (fixed)	0.0 (fixed)	45.2±0.8±0.6
$K^*(1410)^+$	2.29±0.37±0.20	86.7±12.0±9.6	3.7±1.1±1.1
$K^+\pi^0(S)$	1.76±0.36±0.18	-179.8±21.3±12.3	16.3±3.4±2.1
$\phi(1020)$	0.69±0.01±0.02	-20.7±13.6±9.3	19.3±0.6±0.4
$f_0(980)$	0.51±0.07±0.04	-177.5±13.7±8.6	6.7±1.4±1.2
$[a_0(980)^0]$	[0.48±0.08±0.04]	[-154.0±14.1±8.6]	[6.0±1.8±1.2]
$f_2'(1525)$	1.11±0.38±0.28	-18.7±19.3±13.6	0.08±0.04±0.05
$K^*(892)^-$	0.601±0.011±0.011	-37.0±1.9±2.2	16.0±0.8±0.6
$K^*(1410)^-$	2.63±0.51±0.47	-172.0±6.6±6.2	4.8±1.8±1.2
$K^-\pi^0(S)$	0.70±0.27±0.24	133.2±22.5±25.2	2.7±1.4±0.8

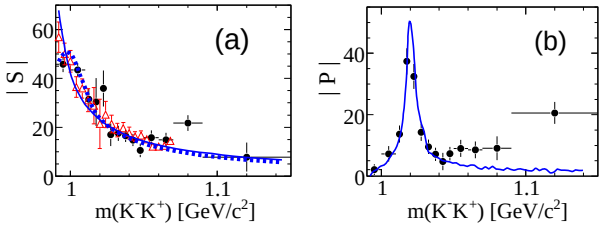

Figure 10: *BABAR*. The phase-space-corrected K^-K^+ S- and P-wave amplitudes, $|S|$ and $|P|$ respectively, in arbitrary units, as functions of the invariant mass compared with results from other analyses.

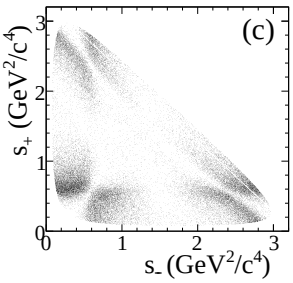

Figure 11: *BABAR*. The 2-dimensional $(s_+ = m^2(\pi^+\pi^0), s_- = (m^2(\pi^-\pi^0))$ distribution of $D^0 \to \pi^+\pi^-\pi^0$.

Table 9: Results from searches for CP violation in Dalitz plot analyses from different experiments.

Decay mode	$\mathcal{A}_{CP}$(%)
$D^0 \to K^-\pi^+\pi^0$	-3.1 ± 8.6
$D^0 \to K^+\pi^-\pi^0$	$+9^{+22}_{-25}$
$D^0 \to K^0_S\pi^+\pi^-$	$-0.9 \pm 2.1^{+1.0+1.3}_{-4.3-3.7}$
$D^0 \to \pi^+\pi^-\pi^0$	$+1^{+9}_{-7} \pm 9$
$D^+ \to K^+K^-\pi^+$	$-0.4 \pm 2.0^{+0.2}_{-0.5}$

Dalitz plot analysis and search for CP violation.

In the limit of CP conservation, charge conjugate decays will have the same Dalitz plot distribution. CP violation expected in Cabibbo-Suppressed charm decays. The integrated CP violation across the Dalitz plot is determined from:

$$\mathcal{A}_{CP} = \int \frac{|\mathcal{M}|^2 - |\overline{\mathcal{M}}|^2}{|\mathcal{M}|^2 + |\overline{\mathcal{M}}|^2}\, dm^2_{ab}\, dm^2_{bc} \Big/ \int dm^2_{ab}\, dm^2_{bc}\,,$$

where $\mathcal{M}$ and $\overline{\mathcal{M}}$ are the D^0 and $\overline{D}^0$ Dalitz plot amplitudes. Table 9 shows results from different experiments. No evidence of CP violation has been observed. The $D^0 \to \pi^+\pi^-\pi^0$ Dalitz plot from *BABAR* ($\approx$ 45 000 events) is shown in fig. 11 and is dominated by intermediate ρ resonances. A direct comparison of the efficiency-corrected and background-subtracted DPs for $D^0$and $\overline{D}^0$events is the simplest way to look for CPV. *BABAR* has performed this analysis [38] using $D^0 \to K^+K^-\pi^0$ and $D^0 \to \pi^+\pi^-\pi^0$ decays. Figure 12 shows the normalized residuals Δ in DP area elements, where

$$\Delta = \left(n_{\overline{D}^0} - R \cdot n_{D^0}\right) / \sqrt{\sigma^2_{n_{\overline{D}^0}} + R^2 \cdot \sigma^2_{n_{D^0}}}\,, \qquad (12)$$

and n denotes the number of events in a DP element and σ its uncertainty. The factor R, equal to 0.983 ± 0.006 for $\pi^-\pi^+\pi^0$ and 1.020 ± 0.016 for $K^-K^+\pi^0$, is the ratio of the number of efficiency-corrected $\overline{D}^0$to D^0events. This is introduced to allow for any asymmetry in the production cross section due to higher order QED corrections or in the branching fractions for $D^0$and $\overline{D}^0$decay to the same final state.

They calculate $\chi^2/\nu = (\sum_{i=1}^{\nu} \Delta_i^2)/\nu$, where ν is the number of DP elements: 1429 for $\pi^-\pi^+\pi^0$ and 726 for $K^-K^+\pi^0$. In an ensemble of simulated experiments with no CPV, we find the distribution of χ^2/ν values to have a mean of 1.012 $\pm$ 0.001 (1.021 $\pm$ 0.002) and an r.m.s. of 0.018 (0.036) for $\pi^-\pi^+\pi^0$ ($K^-K^+\pi^0$). The measured value in the data is 1.020 for $\pi^-\pi^+\pi^0$ and 1.056 for $K^-K^+\pi^0$, so they obtain a one-sided Gaussian confidence level (CL) for consistency with no CPV of 32.8% for $\pi^-\pi^+\pi^0$ and 16.6% for $K^-K^+\pi^0$.

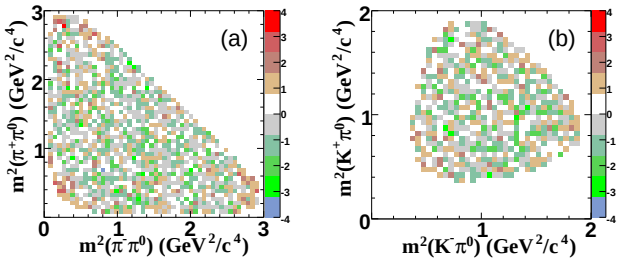

Figure 12: *BABAR*. Normalized residuals in Dalitz plot elements, defined in Eq. 12, for (a) $D \to \pi^-\pi^+\pi^0$ and (b) $D \to K^-K^+\pi^0$.

Conclusions.

Charm meson multi-body decays are crucial to determine light strong interaction bound states. The nature of such mesons is still unclear, but more information is emerging from high statistics Dalitz analysis of D decays. In the future multi-channels analyses may be the way to go to identify underline structure of the light mesons. For instance a measurement of the couplings of the S-wave in various D_s decays can help in interpreting the $f_0(980)$ as two di-quark bound states [39]. Isobar model analyses have several limitations: a) violation of unitarity for broad overlapping resonances and b) the production of possible fake states. K-matrix approaches, on the other hand, rely entirely on results from past experiments. High statistics Model Independent Partial Wave Analyses and direct Partial Wave Analyses in charm decays provide very useful tools to perform new measurements of amplitudes and phases in very clean conditions.

References

[1] M. Bauer, B. Stech and M. Wirbel, Z. Phys. C **34**, 103 (1987).

[2] R.H. Dalitz, Philos. Mag. **44**, 1068 (1953).

[3] J.L. Rosner, Phys. Rev. **D74**, 076006 (2006); M.R. Pennington, Int. J. Mod. Phys. **D21**, 5503 (2006); D. V. Bugg, Phys. Lett. **B632**, 471 (2006).

[4] E.M. Aitala *et al.*(E791 Collaboration), Phys. Rev. Lett. **89**, 121801 (2002).

[5] E.M. Aitala *et. al* (E791 Collaboration), Phys. Rev. Lett. **86**, 770 (2001).

[6] F. E. Close and N. A. Tornqvist, J. Phys. **G28**, R249 (2002).

[7] Charge conjugation is always implied throughout the paper.

[8] A. Giri, Y. Grossman, A. Soffer, and J. Zupan, Phys. Rev. **D68**, 054018 (2003).

[9] B.Aubert *et al.* (BaBar Collaboration), Phys.Rev.**D 78** 034023 (2008).

[10] S.J. Lindenbaum and R.M. Sternheimer, Phys. Rev. **105**, 1874 (1957); M.G. Olsson and G.V. Yodh, Phys. Rev. **145**, 1309 (1966); D.J. Herndon, P. Söding, and R.J. Cashmore, Phys. Rev. **D11**, 3165 (1975).

[11] J.M. Blatt and W.F. Weisskopf, Theoretical Nuclear Physics, John Wiley & Sons, New York, 1952.

[12] W. -M. Yao *et al.* (PDG), J. Phys. **G33**, 1 (2006).

[13] A. Poluetkov *et al.* (Belle Collaboration), Phys. Rev. D **70**, 072003 (2004);

[14] S. Kopp *et al.* (CLEO Collaboration), Phys. Rev. D **63**, 092001 (2001).

[15] E. P. Wigner, Phys. Rev. 70 (1946) 15; S. U. Chung *et al.*, Ann. Physik 4 (1995) 404.

[16] I. J. R. Aitchison, Nucl. Phys. **A189**, 417 (1972).

[17] V. V. Anisovich and A. V. Sarantev, Eur. Phys. Jour. A **16**, 229 (2003).

[18] G.Bonvicini *et al.* (CLEO Collaboration), Phys. Rev. D 76, 012001 (2007).

[19] P.L. Frabetti *et al.* (E687 Collaboration), Phys. Lett. B **407**, 79 (1997).

[20] J.C. Anjos *et al.* (E691 Collaboration), Phys. Rev. Lett. **62**, 125 (1989).

[21] J.M. Link *et al.* (FOCUS Collaboration), Phys. Lett. B **585**, 200 (2004).

[22] J.A. Oller, Phys. Rev. D **71**, 054030 (2005).

[23] S.M. Flatté, Phys. Lett. **B38**, 232 (1972); S.M. Flatté, CERN/EP/PHYS 76-8, 15 April 1976; S.M. Flatté Phys. Lett. B.**63**, 224 (1976).

[24] M. Ablikim *et al.* (BES Collaboration), Phys. Lett. B **607**, 243 (2005).

[25] J. Schechter, Int.J.Mod.Phys. **A20**, 6149 (2005).

[26] N.N. Achasov and G.N. Shestakov, Phys. Rev. **D 67**, 114018 (2003).

[27] J. M. Link *et al.* [FOCUS Collaboration], Phys. Lett. B **653**, 200 (2007).

[28] G. Bonvicini *et al.* (CLEO), Phys. Rev. D **78**, 052001 (2008).

[29] D. Aston *et al.* (LASS), Nucl. Phys. **B296**, 493 (1988); W.M. Dunwoodie, private communication.

[30] E.M. Aitala *et al.* (E791 Collaboration), Phys. Rev. **D73**, 032004 (2006);

[31] B. Aubert *et al.* (BaBar Collaboration), Phys. Rev. **D79**, 032003 (2009)

[32] E. M. Aitala *et al.* [E791 Collaboration], Phys. Rev. Lett. **86**, 765 (2001).

[33] J. M. Link *et al.* [FOCUS Collaboration], Phys. Lett. B **585**, 200 (2004).

[34] R.E. Mitchell *et al.* (CLEO Collaboration), arXiv:0903.1301.

[35] B. Aubert *et al.* (BaBar Collaboration), Phys. Rev. **D72**, 052008 (2005).

[36] S.U. Chung, Phys. Rev. **D56**, 7299 (1997).

[37] B.Aubert *et al.* (BaBar Collaboration), Phys. Rev. **D76**, 011102 (2007).

[38] B. Aubert *et al.* (BaBar Collaboration), Phys. Rev. **D78**, 051102 (2008).

[39] L. Maiani, A. D. Polosa and V. Riquer, Phys. Lett. B **651**, 129 (2007).